

# Fabrication of a Mechanical Antireflection Switch for Fiber-to-the-Home Systems

James A. Walker, Keith W. Goossen, and Susanne C. Arney

**Abstract**—We present the methods used to fabricate a micromechanical silicon optical modulator for use in a fiber-to-the-home applications. We emphasize the efforts made to realize a practical, robust, manufacturable, and easily packaged device. In addition, recent speed, temperature stability, and reliability results are presented. Rise and fall times of 132 and 125 ns, respectively, have been observed in response to a square wave drive signal. The device has been temperature cycled from  $-50^{\circ}\text{C}$  to  $90^{\circ}\text{C}$  and shown greater than 10-dB optical contrast ratio over this temperature range. Finally, the device has been cycled at 500 kHz for a period of nearly two months (two-trillion cycles) without a noticeable loss in performance. [134]

## I. INTRODUCTION

THERE has been much recent emphasis on providing the world with an information super highway. It is believed by many that this will consist of a backbone of fiber optics that will extend throughout the network, all the way to the subscriber location or home. Recent work in the fiber-optics community has focused on providing a fiber-to-the-home (FTTH) system, which can provide the bandwidth required to enable the high-performance services promised by proponents of the information superhighway. In some system configurations, an optical modulator is used at the subscriber interface to imprint outgoing information on an incoming signal and reroute it onto a fiber back to the central office [1], [2]. Some advantages of using an optical modulator for this purpose are the maintenance of wavelength coherence of the signal, reliability of the optical device, temperature insensitivity, and, most notably, cost. We present here an optical modulator based on microelectromechanical systems (MEMS) principles that incorporates a moving dielectric film to provide optical modulation. We call this device a mechanical antireflection switch (MARS) device [3]. Attributes of the MARS device include high speed, high contrast compared to other surface normal modulators, temperature insensitivity, polarization independence (due to its surface normal nature), and low cost. In [3], we presented a device that illustrated the modulator principles, but was fabricated without emphasis on reliability or yield. Here we present fabrication sequences that result in practical, robust devices and demonstrate high reliability.

Manuscript received December 22, 1994; revised December 21, 1995.  
Subject Editor, K. Petersen.  
J. A. Walker and K. W. Goossen are with AT&T Bell Laboratories, Holmdel, NJ 07733 USA.  
S. C. Arney is with AT&T Bell Laboratories, Murray Hill, NJ USA.  
Publisher Item Identifier S 1057-7157(96)02082-3.

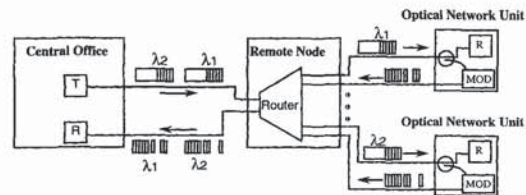


Fig. 1. Representation of RITE-net architecture [2].

## A. Fiber-to-the-Home Systems

The FTTH systems under consideration here are packet-switched data networks. In this type of system, information is divided into discrete blocks of information of 48 bytes, called packets. These packets are sent serially through the network and received at their destination, where they are reconstructed into the complete information stream. A schematic representation of one such network, called RITE-Net [2], is shown in Fig. 1.

In RITE-Net, each packet traveling from the central office consists of a front half, which contains the downstream information going to the subscriber. The second half of the packet consists of a steady stream of light. Many channels of information are contained in the signal leaving the central office (CO) by means of wavelength division multiplexing. At the remote node, these multiple wavelengths are separated by means of a passive element known as a Dragone router [4], and each wavelength then travels separately to its intended optical network unit (ONU). The ONU could be an individual subscriber node (home) or a group of up to four. At the ONU, the packet travels through a fiber splitter, sending the downstream signal to a receiver and simultaneously sending the packet to an optical modulator. The modulator blanks out the first half of the packet (although this is not required) and imprints the upstream data on the CW light in the second half of the packet. This data then travels back to the remote node where the Dragone router multiplexes it with the other wavelengths and they are sent back to the central office again. Since there are relatively few central offices compared to the ONU's, it is possible to use high-performance (i.e., expensive) transmitters and receivers in the CO's. However, to provide the same level of component at every ONU would be prohibitively expensive, so it is therefore necessary to provide an inexpensive alternative able to provide the most basic service. Bandwidth requirements for several levels of services are shown in Table I.

TABLE I  
BANDWIDTH REQUIREMENTS FOR VARIOUS LEVELS OF TELEPHONY SERVICES

Service Bandwidth Requirements	
Standard telephone service (DS0)	64 kBit/s
Video conference service (6 DS0s)	384 kBit/s
Compressed video transmission	1.5-4.5 MBit/s
Local area computer networks (LANs)	10 MBit/s
Uncompressed video transmission	100 MBit/s

A great many consumers will only be initially interested in maintaining the type of telephone service presently available, which requires only 64 kBits/s bandwidth. Although it is necessary to upgrade the network to provide higher-level services, every customer cannot be charged to pay for that upgrade if they are not utilizing the higher bandwidth. The subscriber who wishes higher bandwidth services will be willing to pay a surcharge to obtain higher-performance-level components. Volumes in the United States for the general service units are estimated to be roughly 100 million, given the present number of subscribers to the telephone network. A five-year deployment would therefore entail fabricating and installing roughly 100 000 units per day over the five years. Again, this underscores the need for a cost effective and reliable solution. We are proposing as one possible solution the modulator described here.

## II. MECHANICAL ANTIREFLECTION SWITCH (MARS) DEVICE

The MARS device is a surface-normal modulation device based on a moving antireflection film as described below. Examples of other devices based on vertically moving mechanical films can be found in literature, such as vertically moving gratings [5], moving metallic reflectors [6], and variable air-gap Fabry-Perot structures [7]. For a fiber-to-the-home application it is necessary that the modulator have wide fabrication tolerance, high speed, wide optical spectrum, and low total packaged cost. Although the TI digital micromirror device can form a very good display element, it is unlikely to achieve the Mbt/s response times required here. By the very nature of their modulation mechanisms, the deformable light valve and variable Fabry-Perot device suffer from a narrow optical spectrum and high fabrication complexity, which leads to high fabrication cost. As will be described here, the MARS device can satisfy all of the above operating requirements as well as promise very low fabrication cost.

The operating principle of the MARS device is fairly simple. The device is based on optical interference effects between a dielectric film suspended above a substrate and the substrate. Optical antireflection films are widely used in the optics field. An antireflection film is formed by a dielectric film of a

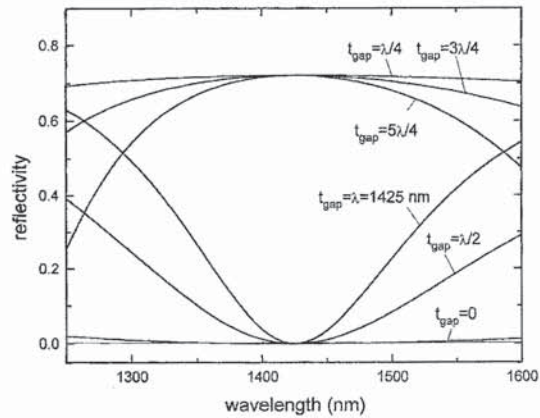


Fig. 2. Modeled optical spectrum for a suspended 1950-Å-thick film of silicon nitride.

thickness equal to  $1/4$  wavelength ( $\lambda$ ) of the incident light and with a refractive index equal to the square root of that of the substrate. If this film is instead suspended above the substrate by an air gap of  $\lambda/4$ , it then becomes a nearly perfect reflector. More generally, if the air gap is of thickness  $\frac{m\lambda}{4}$ , there exists an antireflection state for  $m$  even, and for  $m$  odd there is a reflecting state. Therefore, the reflectivity state of a device can be changed from reflecting to nonreflecting by a change in air gap of  $\lambda/4$ . For the most basic MARS device, we create a silicon nitride membrane suspended above a silicon substrate by  $\lambda/4$  using surface micromachining techniques. The nitride film is then electrostatically attracted toward the substrate creating a  $\lambda/4$  antireflection condition upon contact. The  $m = 1$  case is the most fundamental and provides the largest optical spectrum, as shown in Fig. 2. However, as mentioned earlier, any structure that has an initial air gap of thickness  $\frac{m\lambda}{4}$  where  $m$  is odd would have similar operating characteristics at a given wavelength. Due to the nature of the intended application, one of our goals is to strive for a wide optical spectrum with contrast ratio greater than 10:1. A model of the optical spectrum for a suspended film of 1950-Å-thick silicon nitride with a refractive index of 1.87 is shown in Fig. 2. One can see that for the  $\lambda/4$  case, contrast ratios in excess of 25:1 are possible for wavelengths ranging from below 1300 nm to greater than 1600 nm. This broad spectral width makes this device useful at both typical operating wavelengths used in fiber-optics communications systems—1320 and 1560 nm. For the case where  $m$  is increased to three, the optical bandwidth is considerably narrower. The contrast ratio at a given center wavelength, however, would still be very high. The basic operation of the MARS device is illustrated in Fig. 3.

Our modeling indicates that the deflection over the optical window is within 5% of the design value. Plane wave modeling shows that the contrast at the center wavelength remains greater than 180:1. Since our actual contrast is less than this (20:1), deflection does not appear to introduce significant

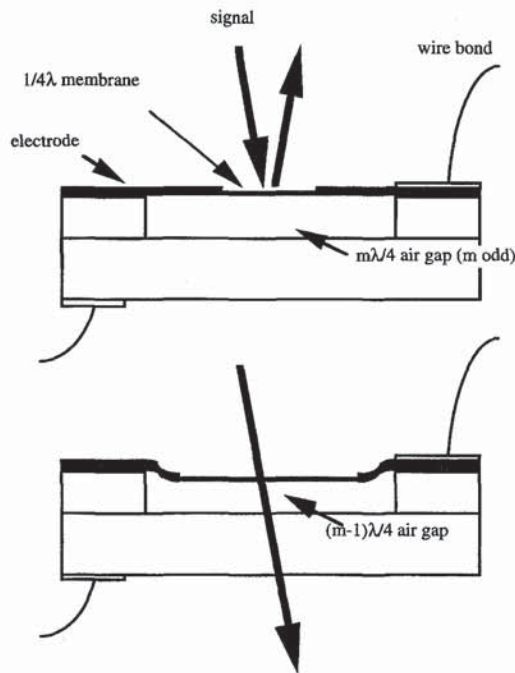


Fig. 3. MARS device operation.

degradation by itself. In fact, curvature of the optical window may actually help since we operate with the deflected state as the antireflection state, and so it will tend to deflect light away from the optical fiber and augment contrast.

Fig. 4 shows the model of the optical spectrum for a device having a suspended film which is a composite of 1000 Å of polysilicon and 1950 Å of silicon nitride with an index of 1.87. As one can see, the performance is very similar in nature to that of the single film [3]. This is because the polysilicon layer is assumed to have the same refractive index as that of the silicon substrate, so that when the membrane is in contact with the substrate (or for any  $m$  even), the structure is optically identical to the nitride-only membrane. Since the poly-silicon layer is  $\lambda/4$  thick, for  $m$  odd it actually augments the reflectivity, leading to enhanced modulation. As will be discussed below, the use of this composite film structure provides some flexibility in tailoring mechanical properties without affecting optical performance.

### III. FABRICATION

The fabrication of the MARS device is complicated by the interdependent nature of the mechanical properties, optical performance requirements, and electrical performance of the device. For a given silicon nitride film deposited using plasma-enhanced chemical vapor deposition (PECVD), the residual film stress cannot be tailored without affecting the film's refractive index. Also, changes in film stress affect

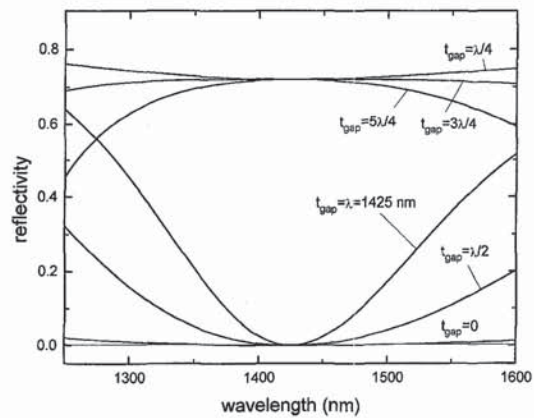


Fig. 4. Modeled optical spectrum for a suspended composite film of 1000-Å-thick polysilicon and 1950-Å-thick silicon nitride.

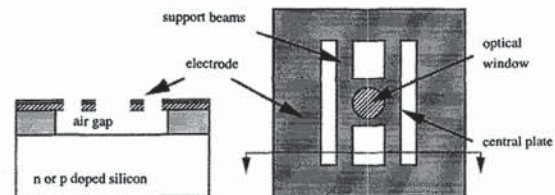


Fig. 5. Topographical and side views of a typical MARS device.

the required drive voltage for actuation and the ability to obtain reasonable yield after the sacrificial layer etch. For the simplest film structure consisting of an aluminum sacrificial film and silicon nitride membrane, these constraints provide a significant challenge.

The structure of a representative MARS device is shown in Fig. 5. The mechanically active area of the device is defined as the area released from the substrate and consists of the central plate supported by thin support beams. An opening in the electrode material on the central plate defines the optical window of the device. Obviously, variations of this structure are possible and many have been fabricated. For the purposes of this paper, however, we are confining our discussion to this basic structure.

In the simplest fabrication method, we begin by depositing a  $3\lambda/4$ -thick film (1.16  $\mu\text{m}$  thick for an operating wavelength of 1560 nm) of E-gun evaporated aluminum on a doped silicon substrate. A film of PECVD silicon nitride is then deposited on the aluminum using 200 sccm of 2% silane in nitrogen, 900 sccm of pure nitrogen, and 3 sccm ammonia at 250°C, 60 mW/cm<sup>2</sup> and 900 mTorr. This results in a 1950-Å-thick silicon nitride film with an index of  $1.9 \pm 0.05$ , which is under moderate tensile strain. This film is patterned using an SF<sub>6</sub>:CCl<sub>2</sub>F<sub>2</sub> reactive ion etch to form the devices. Electrodes are then added using lift-off of 55 Å of titanium and 1000 Å of gold. The structure is then released in a 60°C bath of commercially available aluminum etch and rinsed in flowing

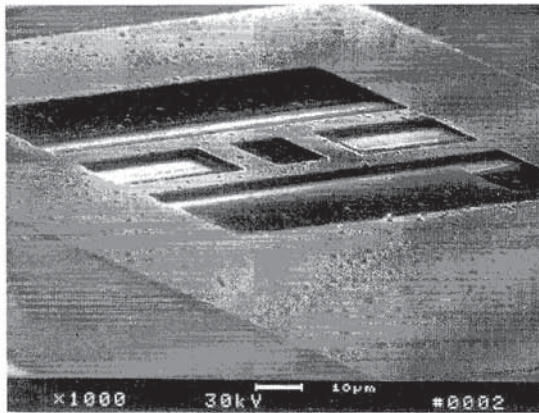


Fig. 6. Completed MARS device.

DI water for five minutes. A sequential exchange of water with methanol is then used and the devices are left to air dry. An SEM photograph of a completed, released device is shown in Fig. 6.

While the aluminum/PECVD nitride structure is convenient from the point of view of equipment capability and cost, this choice of material system does present some problems. Aluminum, while easily deposited and etched, is a less than ideal sacrificial film for this device. When depositing thicknesses approaching  $1\ \mu\text{m}$ , the surface of aluminum can become quite rough and hillocks of greater than  $1\ \mu\text{m}$  can form. We have explored the use of both thermally evaporated aluminum and E-gun evaporated aluminum. The surface structure of the E-gun aluminum was found to have a considerably smoother surface with an average surface roughness of  $\pm 60\ \text{\AA}$ , as opposed to  $\pm 250\ \text{\AA}$  for thermal aluminum. These roughness values are for as deposited films. During PECVD nitride deposition they become rougher due to the heating and induced stress associated with the PECVD process.

In addition, because we are using PECVD silicon nitride, pinhole formation in the dielectric is a potential problem. When coupled with the surface roughness of the aluminum, pinhole density becomes an even greater issue. From Fig. 3, one can see that if the sacrificial film is a conductor, the electric field for a given voltage is much higher under the wire bond pad area of the device than in the moving area. Therefore, the existence of pinholes in the nitride or aluminum hillocks under the nitride can lead to shorting of the electrodes and failure of the device. In addition to changing the sacrificial film, we have tried two approaches to circumventing this problem. 1) We have added a  $1000\text{-\AA}$ -thick film of evaporated silicon monoxide under the wire bond pad area as an extra insulator. 2) We are patterning the aluminum so that it only exists in the mechanically active area of the device. We have found both methods can be successful, however the aluminum island approach requires a conformal silicon nitride and complicates the mechanical properties of the device.

In our first attempts to fabricate the device, we chose an electrode structure of a  $50\text{-\AA}$ -thick layer of chrome followed

by a  $1000\text{-\AA}$ -thick film of pure gold. The purpose of the chrome is to aid the adhesion of the gold to the silicon nitride. Upon removal from the aluminum etch used to release the membranes, the contacts appeared to be good. While the devices were being electrically actuated, however, bubbling under the gold was observed. The bubbling would continue until finally the electrode, and therefore the device, would fail. The same electrical signal was applied to devices that had not been released with no observation of this effect. It was concluded that the aluminum etch was attacking the chrome adhesion film during release, leading to failure. We have subsequently switched to titanium for the adhesion film, and this has resulted in a robust, reliable electrode.

Since the structure is conceptually so simple, there are a myriad of other material systems from which to choose. Most of our work, however, has been with the aluminum/nitride structure due to available technology. We are presently evaluating the use of other metals (e.g., copper), polymers (e.g., polyimide), and highly HF-soluble glasses as the sacrificial film. Obviously, as with any micromachining process, etch selectivity is a concern. This is especially true here, since any change in the nitride membrane thickness would change the optical properties of the device.

Another material system we have explored consists of a sacrificial layer of silicon dioxide and a composite structural layer of a  $1000\text{-\AA}$ -thick film of polysilicon and a  $1950\text{-\AA}$ -thick film of silicon nitride. There are several advantages to this type of structure. 1) The mechanical properties of the membrane can be decoupled from its optical performance, since the stress in the polysilicon film can be tailored independently of any properties of the subsequent silicon nitride film. When using just a nitride film, the residual stress in the film and its refractive index are coupled. 2) A local oxidation method (LOCOS) can be used to form an oxide island under the desired mechanically active region only. 3) The polysilicon can be made arbitrarily thick outside of the optical window, making the structure less compliant and making the release procedure more reliable.

To this point, stiction upon release of the polysilicon/nitride structure has been a problem. In part, this is due to our choice of  $\lambda/4$ -thick oxide films for the sacrificial layers as well as the high compliance of the  $1000\text{-\AA}$ -thick polysilicon film. We are presently exploring the use of a  $3\lambda/4$  gap as well as adding thicker structural polysilicon outside of the optical window. We are also exploring the use of supercritical  $\text{CO}_2$  release procedures reported elsewhere [8].

Because device cost is of such paramount importance for our intended application, we have kept our fabrication methods as simple as possible. Estimates of fabrication costs are in the range of a few pennies per device. We feel that packaging costs will be the dominant cost for any completed system. Fortunately, in this case the packaging costs should also be relatively low since the device is a surface normal device of very small size. In addition, the optical window can be made much larger than the core of a standard single-mode fiber resulting in alignment tolerances of tens of microns. Finally, the device is polarization independent. All of these factors should result in very low-cost packaging.

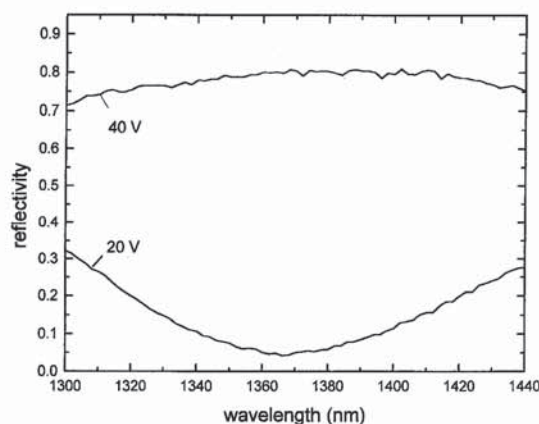


Fig. 7. Measured optical spectra for a  $1\lambda$ -thickness air gap device.

#### IV. RESULTS

All of the results discussed here were obtained using devices fabricated with the aluminum/PECVD nitride process. As mentioned above, variations of beam width, length, and central plate size have been explored. The central plate has been varied from  $10 \times 10 \mu\text{m}$  to  $100 \times 100 \mu\text{m}$ . The beam width has been varied from  $2\text{--}21 \mu\text{m}$ , and beam lengths range from  $5\text{--}75 \mu\text{m}$ . A model of the mechanical performance is being developed in order to optimize the device structure.

We have fabricated samples for operating wavelengths ranging from  $1300\text{--}1560 \text{ nm}$ , determined primarily by the thickness of the sacrificial film. The spectral bandwidth for an aluminum/nitride device with a zero-bias air gap of roughly  $1.37 \mu\text{m}$  is shown in Fig. 7. The spectra for bias conditions of 20 and 40 V show a measured contrast ratio of roughly 15:1 at  $1370 \text{ nm}$  for this device. Using a minimum contrast ratio of 10:1, the spectral width of the device is approximately  $40 \text{ nm}$ , as would be expected based on the modeling shown in Fig. 3 showing that as the air gap thickness is increased, the spectral width decreases.

Since a device in service in a FTTH system would be subjected to temperatures ranging from summer in Arizona to winter in Alaska, it was necessary to examine the temperature variation of the operating parameters. Therefore, the ambient temperature of this device was varied from  $-50^\circ\text{C}$  to  $90^\circ\text{C}$  in order to determine what effect this would have on the spectral response. DC measurements were done in vacuum in order to avoid the formation of frost on the device. As can be seen in Fig. 8, although there is a shift in central wavelength, the contrast ratio remains relatively high over the desired range of wavelengths. We believe the shift is due to thermal expansion of materials and changes in the air gap due to temperature variant stresses. It may be possible to alleviate some of these issues with modifications to the device structure, as well as by broadening the optical bandwidth of the device by reducing the air gap.

We performed speed measurements on one of the  $m = 4$  devices (air gap =  $\lambda$ ) with a  $30 \times 30 \mu\text{m}$  central plate,  $20\text{-}\mu\text{m}$ -long  $\times$   $5\text{-}\mu\text{m}$ -wide support beams, and a drive voltage of

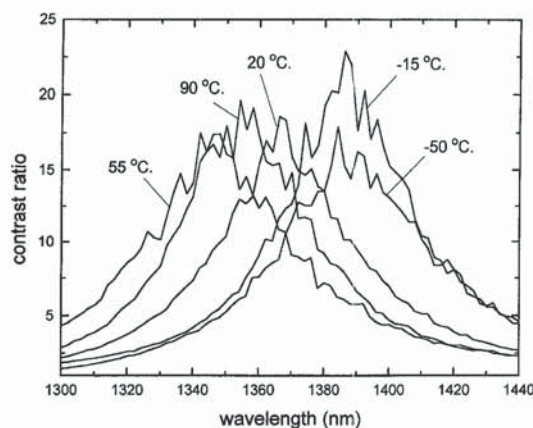


Fig. 8. Modulator contrast ratio spectra at temperatures from  $-50^\circ\text{C}$  to  $90^\circ\text{C}$ .

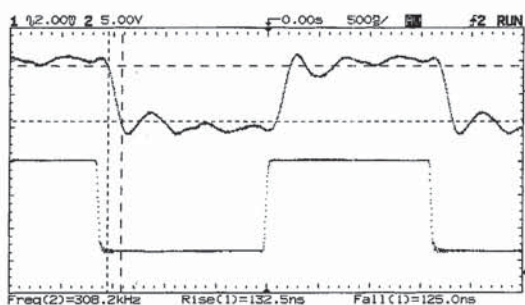


Fig. 9. Temporal response to a square wave drive signal.

25 V. The electrode area extends down the support beams and covers the outer edge of the central plate, leaving an optical window of  $20 \times 20 \mu\text{m}$ . Since the required drive voltage scales as the inverse of the square of air gap, the drive voltage can be significantly reduced by going to an air gap of  $m = 1$  or using a tiered structure that has an electrode spacing of  $m = 1$ , but a different optical window spacing.

Device response to a square wave drive pulse train is shown in Fig. 9, where rise and fall times for the device are 132 and 125 ns (as measured in a standard laboratory environment), respectively. For a data communications system, these translate to a bitrate greater than 2 Mbit/s. Devices from the same wafer with central plates of  $40 \times 40 \mu\text{m}$  were tested and found to have rise and fall times of roughly 350 ns. Similar devices were tested in both an ambient air environment and in vacuum, and it was found that air damping is a dominating factor for device speed. The trace for the  $20 \times 20 \mu\text{m}$  device shows some ringing due to an underdamped oscillator condition. A clean signal can theoretically be obtained through the use of simple signal-conditioning techniques [3].

A  $40 \times 40 \mu\text{m}$  plate device was placed in a measurement setup and run at 500 kHz for 50 days or over 2 trillion cycles.

# Explore Litigation Insights

Docket Alarm provides insights to develop a more informed litigation strategy and the peace of mind of knowing you're on top of things.

## Real-Time Litigation Alerts



Keep your litigation team up-to-date with **real-time alerts** and advanced team management tools built for the enterprise, all while greatly reducing PACER spend.

Our comprehensive service means we can handle Federal, State, and Administrative courts across the country.

## Advanced Docket Research



With over 230 million records, Docket Alarm's cloud-native docket research platform finds what other services can't. Coverage includes Federal, State, plus PTAB, TTAB, ITC and NLRB decisions, all in one place.

Identify arguments that have been successful in the past with full text, pinpoint searching. Link to case law cited within any court document via Fastcase.

## Analytics At Your Fingertips



Learn what happened the last time a particular judge, opposing counsel or company faced cases similar to yours.

Advanced out-of-the-box PTAB and TTAB analytics are always at your fingertips.

## API

Docket Alarm offers a powerful API (application programming interface) to developers that want to integrate case filings into their apps.

## LAW FIRMS

Build custom dashboards for your attorneys and clients with live data direct from the court.

Automate many repetitive legal tasks like conflict checks, document management, and marketing.

## FINANCIAL INSTITUTIONS

Litigation and bankruptcy checks for companies and debtors.

## E-DISCOVERY AND LEGAL VENDORS

Sync your system to PACER to automate legal marketing.